EAI Endorsed Transactions
on Energy Web
Research Article EAI.EU

An Early Warning Method for Abnormal Fluttering Behavior in Transmission Lines Based on Deep Binocular Vision

Zhimeng Zhang[1,*], Jie Liu[1], Cuiying Sun[1], Xiaoyu Yi[1], Yixin Wang[1]

[1]Electric Power Research Institute of State Grid Hebei Electric Power Co., Ltd., Shijiazhuang, 050021, China

Abstract

Under adverse weather conditions, ice accumulation and strong winds cause low-frequency and high-amplitude swaying of transmission lines, increasing the risk of wire fatigue, hardware damage, and tower collapse, posing a threat to the safety of the power grid. The existing monitoring methods suffer from inaccurate 3D spatial data acquisition, leading to errors in edge detection, difficulty in suppressing background interference, insufficient feature extraction, and reduced accuracy in detecting abnormal oscillations. Therefore, this article proposes a warning method based on deep binocular vision, which captures three-dimensional data with a stereo camera and converts it into two-dimensional images. Mathematical morphological operators are used to determine the edge of the transmission line, solving the problem of inaccurate edge detection. The morphological edge results are input into the ResNet LSTM network to suppress background noise and extract features. Finally, compare the detection results with the actual values to achieve multi-level alarms. The experiment shows that this method is efficient and accurate, with a detection efficiency of 0.958-0.968. Improved the reliability of early warning.

Keywords: Deep Binocular Vision, Power Transmission Lines, Morphological Edges, Background Suppression, Flutter Anomaly Behavior, Early Warning Method.

Received on 07 September 2025, accepted on 21 December 2025, published on 04 May 2026

doi: 10.4108/ew.12827

1. Introduction

Transmission lines are the key to power transmission, and their safety is related to national energy and socio-economic development [1]. However, the shaking of power lines caused by severe weather conditions such as ice accumulation and strong winds seriously threatens the safety of the power grid. The vibration generated by the shaking can cause damage to the wires, hardware, and even lead to accidents such as tower collapse and short circuits, resulting in significant losses [2]. The current warning methods face numerous challenges in data collection, feature extraction, and behavior detection. Inaccurate 3D data collection affects edge detection, and traditional methods are susceptible to background noise interference, which affects the accuracy of identifying abnormal vibrations. Therefore, there is an urgent need to explore more reliable warning methods to solve these problems [3].

The expansion of the power grid scale and frequent occurrence of extreme weather pose challenges to the safe operation of transmission lines, and real-time monitoring and early warning of abnormal behaviors, such as vibration, have become research hotspots. In existing research, Gonzalez Fernandez et al. [4] identified line flutter through experiments, collected conductor behavior data under different ice shapes, thicknesses, angles of attack, and wind speeds, established dynamic models to simulate wire sway characteristics, and then developed sway pattern recognition models using machine learning

*Corresponding author. Email: 15931090169@163.com

algorithms. However, this method relies on laboratory aerodynamic parameter measurements, making it difficult to simulate complex on-site disturbances, resulting in insufficient noise suppression during feature extraction and affecting the accuracy of flutter recognition. Fayazi et al. [5] proposed a fault detection method based on decision tree (DT) algorithms and fault energy indices to analyze transmission line operational states and classify fault types. This approach utilizes real-time electrical parameters, including voltage, current, and phase angle, from both AC (HVAC) and DC (HVDC) transmission lines. These parameters are fed into a decision tree, enabling rapid fault type detection through feature matching and pattern recognition to distinguish between internal and external transmission line faults. The decision mechanism of this method relies on fixed thresholds, rendering it incapable of adapting to dynamically changing amplitude-frequency characteristics during flicker. When encountering low-frequency, high-amplitude flicker, its detection accuracy sharply declines due to insufficient feature extraction dimensions. Shakiba et al. [6] developed a fault detection approach for transmission lines. By integrating electrical parameters, environmental data, and equipment status data through data fusion methods, they fed this combined information into machine learning models to detect faults. The system outputs risk levels based on fault severity (e.g., fault current magnitude and duration), triggering corresponding early warning response mechanisms. This approach fails to construct the spatial three-dimensional motion trajectory of transmission lines, resulting in complete oversight of morphological edge features in the spatial configuration changes of conductors during swaying. This significantly impacts the accuracy of swaying recognition. Fekri et al. [7] proposed a cascading fault model based on transmission line thermal limits to assess transmission system risks. This model generates fault scenarios constrained by thermal limits, analyzes propagation paths, impact ranges, and system stability for each scenario, and defines vulnerability metrics by integrating system topology and operational constraints to quantify risks. This approach cannot capture three-dimensional motion parameters such as conductor spatial displacement or twist angle, resulting in reduced detection accuracy.

Depth binocular vision technology integrates binocular stereoscopic vision principles with deep learning algorithms. By simulating human binocular perception mechanisms, binocular stereoscopic vision rapidly and accurately acquires three-dimensional depth information of a scene, featuring non-contact operation, high real-time performance, and superior accuracy [8]. Deep learning constructs multi-layer nonlinear neural network models by simulating the structure and function of the human brain's neural networks. It can automatically learn complex feature representations from large-scale data, enabling intelligent analysis and anomaly early warning for transmission line flutter behavior. Therefore, this paper proposes a deep binocular vision-based early warning method for abnormal transmission line swaying behavior. It aims to overcome the limitations of traditional monitoring technologies, achieve high-precision and intelligent monitoring of transmission line swaying states, and provide effective technical support for ensuring the safe and stable operation of power grids.

2. Early Warning of Abnormal Transmission Line Flutter Behaviour

2.1 Transmission Line Flutter State

In power system engineering [9], the geometric structure of overhead transmission lines constitutes a suspension cable system. Determining the initial state and flutter state information of conductors is a prerequisite for implementing flutter monitoring. Cable flutter predominantly occurs under icing conditions, where the geometric surface of conductors is altered. At crosswind speeds of 4–20m/s, the line modifies its aerodynamic characteristics at certain attack angles, causing vertical vibrations. Simultaneously, the torsional characteristics of conductors can also induce vibrations. When their frequencies reach a specific coupling frequency, dancing phenomena occur in transmission lines [10]. A schematic diagram illustrating transmission line dancing is shown in Figure 1.

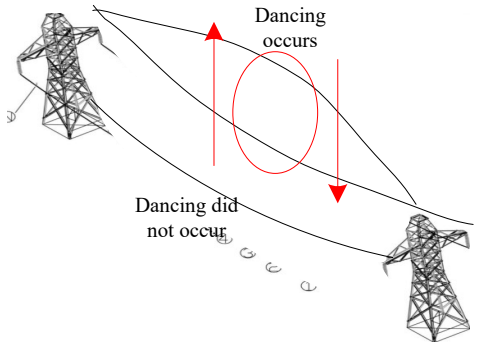

Figure 1. Schematic diagram of transmission line dancing

As illustrated in Figure 1, transmission line dancing is primarily influenced by wind and ice accumulation. Under these effects, the dancing behavior exhibits significant vertical oscillations with large amplitude. As dancing constitutes large-amplitude low-frequency vibration, it subjects conductors to repeated high stresses within short intervals, potentially causing fatigue damage [11], accelerating conductor aging, and reducing service life. Simultaneously, the substantial vibrations generated by swaying transmit to line hardware (such as clamps, hangers, etc.) and insulators. This subjects the hardware to additional impact forces, potentially causing loosening, deformation, or even fracture. Insulators may experience

ceramic cracks or skewing due to vibration stress, which can affect their insulation and mechanical properties. Long-term swaying can also cause the foundation of transmission towers to loosen, structural deformation, and even collapse, posing a threat to the safety of power lines [12]. Therefore, it is necessary to reliably monitor abnormal swaying of the power line and issue timely warnings to prevent faults, protect equipment, reduce line failures, lower the risk of large-scale power outages, ensure a reliable power supply, and encourage maintenance personnel to actively maintain equipment, extending its lifespan and reducing failure rates.

2.2 Overall Architecture of the Binocular Vision and Deep Learning-Based Early Warning Method for Transmission Line Flutter Behavior

This article proposes a vibration warning method for transmission lines based on binocular vision and deep learning, which can reliably identify vibration events. This method consists of two main modules: binocular vision imaging and anomaly warning. The binocular vision imaging module obtains transmission line spatial image data through the binocular vision system [13], and then inputs it into deep learning algorithms to identify vibrations and provide warnings. Its structure is shown in Figure 2.

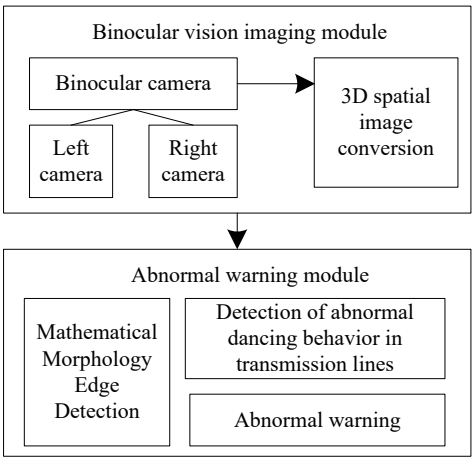

Figure 2. Schematic diagram of power transmission line data acquisition based on binocular vision system

This module consists of two steps: first, the stereo camera collects image data from different perspectives [14], and uses the principle of parallax to calculate three-dimensional information; Further converts spatial data to form easily visualized two-dimensional data, which facilitates technicians to observe changes in the circuit and analyze swaying behavior.

The anomaly warning module consists of three steps: first, perform mathematical morphology edge detection, then use deep learning networks to detect swing anomalies, and finally, integrate the detection results to generate warnings.

2.3 Binocular Vision-Based Power Transmission Line Data Acquisition

To warn of abnormal swaying of transmission lines, it is necessary to obtain their three-dimensional spatial data to capture changes in position. This article uses a binocular vision system to simulate the principle of human eye disparity [15], capturing images of different positions of transmission lines. Through image processing and computer vision algorithm analysis, the three-dimensional position changes of conductors are accurately calculated. The system records the swing cycle of the wire, captures swing images from multiple angles, clearly records ice accumulation, and achieves real-time monitoring of multi-dimensional displacement of the wire, providing key data for swing warning.

A stereo camera captures the same target image from two different angles and calculates the three-dimensional information of the target using the principle of parallax. The imaging principle of a binocular camera is illustrated in Figure 3, where the left and right views represent two imaging planes. $\vec{O}$ and $\vec{O}$ denote the left eye and right eye of the binocular camera, respectively. The baseline distance D is the distance between the projection centers of the two cameras, and f is the camera focal length. Figure 3 shows a schematic diagram of power transmission line data acquisition based on the binocular vision system.

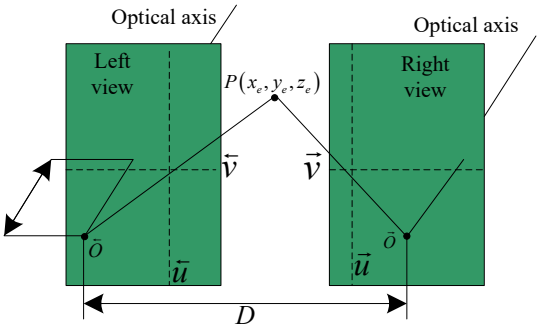

Figure 3. Schematic diagram of power transmission line data acquisition based on binocular vision system

(1) Acquisition of spatial 3D information for power transmission lines:

When both cameras capture the same feature point $P(x_e, y_e, z_e)$ simultaneously, they obtain images of the

point P on their respective left and right imaging planes. Assume the coordinates of P on the left imaging plane are $(\tilde{u},\tilde{v})$, and the coordinates of P on the right imaging plane are $(\vec{u},\vec{v})$. When the imaging planes are perfectly aligned, $\tilde{v}=\vec{v}$ holds. The horizontal coordinate difference $d=|\tilde{u}-\vec{u}|$ is defined as the parallax of this pixel point. Applying the principle of similar triangles, the spatial data results for the transmission line binocular vision can be obtained using the following formula:

$$\begin{cases} x_e = \dfrac{D\tilde{u}}{d} \\ y_e = \dfrac{D\tilde{v}}{d} \\ z_e = \dfrac{Df}{d} \end{cases} \tag{1}$$

From Equation (1), it is evident that under the premise of perfectly horizontal left and right imaging planes, considering the focal length f and baseline distance D as inherent camera parameters, the calculation of the transmission line's 3D coordinates depends solely on the parallax value.

(2) Three-dimensional spatial information conversion:

After obtaining the three-dimensional spatial information of the transmission line using the above formula, this information must be converted into two-dimensional image data. In a binocular vision system [16], the relationship between a three-dimensional object in the world coordinate system and its final two-dimensional image projection can be represented by a geometric model, namely the camera imaging model. Therefore, the three-dimensional spatial information conversion can be performed by combining the internal parameter matrix and external parameter matrix of the stereo camera.

Based on the principles of binocular vision imaging, the physical dimensions of pixels along the x and y axes in the pixel coordinate system are represented by s_x and s_y, respectively. These dimensions, together with f and the pixel coordinates (u_0,v_0), form the internal parameter matrix V of the stereo camera. Meanwhile, the rotation matrix R and translation matrix T of the binocular vision system jointly constitute the external parameter matrix W of the stereo camera. Based on V and W, the relationship between the pixel coordinate system and the world coordinate system is calculated using the following formula:

$$Z_c\begin{bmatrix} u \\ v \\ 1 \end{bmatrix} = \begin{bmatrix} \dfrac{f}{s_x} & 0 & u_0 \\ 0 & \dfrac{f}{s_y} & v_0 \\ 0 & 0 & 1 \end{bmatrix}\begin{bmatrix} R & T \end{bmatrix}\begin{bmatrix} X_o \\ Y_o \\ Z_o \\ 1 \end{bmatrix} \tag{2}$$

Where: (X_w,Y_w,Z_w) represents the world coordinate system; Z_c denotes the perpendicular distance from the spatial point P to the origin of the camera coordinate system; (u,v) is the transformed ideal pixel coordinate.

Using the above formula, the transmission line is transformed from the world coordinate system to the pixel coordinate system, converting its three-dimensional spatial information into a two-dimensional image $I(u,v)$. This image records the morphology, position, and other information of the transmission line in pixels. By processing and analyzing these two-dimensional images, relevant features of the transmission line can be obtained, providing data support for subsequent flutter behavior analysis and anomaly early warning.

2.4 Edge Detection of Transmission Lines Based on Mathematical Morphology

When transmission lines sway, their edge morphology undergoes significant changes. After acquiring the two-dimensional images of transmission lines as described above $I(u,v)$, to ensure the identification and early warning effectiveness of abnormal swaying behaviors, mathematical morphology edge detection operators are employed to determine the edge images of transmission lines. The primary objective is to extract critical parameters—such as length, orientation, and curvature—from the edge image through morphological edge detection. This provides a more reliable basis for identifying distortion and oscillation indicative of abnormal swaying, enabling precise detection of minute oscillations and deformations to uncover anomalous swaying behavior.

The morphological edge detection operator is based on set-theoretic subtraction operations. It primarily performs subtraction between the base operator and the original image. Using $I(u,v)$ as the input image and Q as the structural element, morphological operations are applied to $I(u,v)$ via Q based on the proportion of edge pixels in the image. These operations include dilation, erosion, opening, and closing. The respective operational formulas are:

$$(I\oplus Q)=\max\left\{I(u-\tilde{u},v-\tilde{v})+Q(\tilde{u},\tilde{v})\middle|\begin{matrix}(u-\tilde{u},v-\tilde{v})\in\Omega_I,\\(\tilde{u},\tilde{v})\in\Omega_Q\end{matrix}\right\} \tag{3}$$

$$(I\Theta Q)=\min\left\{I(u+\tilde{u},v+\tilde{v})-Q(\tilde{u},\tilde{v})\middle|\begin{matrix}(u+\tilde{u},v+\tilde{v})\in\Omega_I,\\(\tilde{u},\tilde{v})\in\Omega_Q\end{matrix}\right\} \tag{4}$$

$$I\circ Q=(I\Theta Q)\oplus Q \tag{5}$$

$$I\bullet Q=(I\oplus Q)\Theta Q \tag{6}$$

Where: $Q(\tilde{u},\tilde{v})$ denotes the structural element value; Ω_I and Ω_Q represent the domains of the image and

structural element, respectively; $\oplus$ denotes the dilation operation; Θ denotes the erosion operation; $\square$ denotes the opening operation; $\bullet$ denotes the closing operation.

Based on the above four operations, obtain the $I(u,v)$ multi-directional morphological edge detection result as follows:

$$g_i = \left[\left(I \square \xi_1\right) \bullet \xi_2\right] \oplus Q_i - \left[\left(I \bullet \xi_1\right) \square \xi_2\right] \Theta Q_i \quad (7)$$

Where: g_i denotes the morphological edge detection result of the transmission line image i; ξ_1 and ξ_2 denote the scaling coefficients.

Based on the above content, morphological edge detection of transmission line images can be completed. The result g_i serves as input data for subsequent transmission line flutter anomaly behavior recognition and early warning, thereby better ensuring the judgment of flutter anomaly behavior length, direction, and curvature, and guaranteeing the reliability of the behavior detection results.

2.5 Deep Learning-Based Detection of Abnormal Swaying Behaviour in Transmission Lines

Combining the morphological edge detection results of transmission line images obtained in the preceding subsection g_i enables detection of abnormal swaying behavior. To ensure detection effectiveness, this paper primarily employs ResNet (Residual Network) and Long Short-Term Memory (LSTM) networks from deep learning. By integrating these two networks, a ResNet-LSTM-based transmission line flutter anomaly detection network model is generated. An attention mechanism is introduced into the network for feature extraction, maximizing the detection effectiveness of transmission line flutter anomalies [17]. The model comprises three steps: background suppression processing, feature map extraction, and anomaly detection. Detailed descriptions of each component follow:

(1) Background Suppression Processing: To enhance perception of prominent features in transmission line swaying anomalies, a background suppression module is constructed using the ResNet network. Inputting the g_i into this module extracts the feature map F_g. After convolutional processing, the extracted feature map undergoes pixel-by-pixel summation to form the feature K_c. The formula is:

$$K_c = \psi\left[\beta\left(\omega_c^T F_g\right) + b\right] \quad (8)$$

$$\beta = \kappa \times \frac{g_i - \sigma}{\sqrt{\delta^2 + \varepsilon}} + \eta \quad (9)$$

Where: ψ denotes the activation function; ω_c^T denotes the weight; b denotes the bias term; κ and η denote the translation and scaling parameters; σ and δ denote the mean and standard deviation of g_i; ε denotes the min-constant.

During processing, the above formula combines translation and scaling to enhance edge detection results g_i in transmission line images, effectively suppressing the background regions [18].

(2) Feature Map Extraction:

After extracting K_c through the above steps, an attention mask is formed via the attention mask module M. Multiplying this mask with the feature map F_g yields a new feature map $\tilde{K}$. This process uses the attention mask to supervise the next layer of feature maps, calculated as follows:

$$\tilde{K} = F_g \times \varphi K_c \quad (10)$$

Where: φ denotes the attention mask generation operation.

(3) Dance Anomaly Detection:

After extracting the feature map $\tilde{K}$ through the aforementioned operations, it is fed into an LSTM for dance anomaly detection. The LSTM controls the state of network units by managing the forget gate, input gate, and output gate. This control mechanism enables adaptive learning of sequence features, eliminating unnecessary information while retaining useful information [19]. After $\tilde{K}$ transmission to LSTM, the forget gate uses the Sigmoid activation function to control the unit's state, determining how the previous time state updates the current state to record long-term patterns of dance-related feature changes. The input gate decides which newly received information is updated or stored, determined by the activation value L_i and the memory cell candidate state A. The output gate determines which feature information is permitted to be output, determined by the output activation value ℓ_t and the memory cell output value h_t. Thus, the dance anomaly detection calculation formula at time t is:

$$r_t = \gamma\left(\omega_r h_{t-1} + \omega_K \tilde{K} + b_r\right) \quad (11)$$

$$r_t = \gamma\left(\omega_r h_{t-1} + \varpi_K \tilde{K} + b_r\right) \quad (12)$$

$$L_t = \gamma\left(\omega_r \tilde{K} + \varpi_L h_{t-1} + b_L\right) \quad (13)$$

$$\tilde{A}_t = \lambda\left(\omega_A \tilde{K} + \varpi_A h_{t-1} + b_L\right) \quad (14)$$

$$\ell_t = \gamma\left(\omega_\ell h_{t-1} + \varpi_\ell h_{t-1} + b_\ell\right) \quad (15)$$

$$h_t = \ell_t \times \lambda\left(A_t\right) \quad (16)$$

Where: r_t and ℓ_t represent the gated computation results; γ denotes the Sigmoid activation function; λ indicates the Tanh activation function; ω is the weight matrix; ϖ is the weight vector for the input feature map $\tilde{K}$; b is the

bias vector; A_t is the memory cell state; $\tilde{A}_t$ is the candidate state; h_t is the LSTM output for detecting abnormal flutter behavior in transmission lines.

2.6 Early Warning of Abnormal Transmission Line Flutter Behaviour

The operating environment of transmission lines is complex, influenced by factors such as weather, bird activity, and inherent equipment fluctuations. During detection, some erroneous "false anomaly" signals may be generated. Additionally, transmission lines exhibit significant variations in operational conditions across different seasons and geographic locations, resulting in differing normal sway ranges. Flexibly adapting to these variations ensures the early warning system remains effective under all circumstances. Integrating the findings from the aforementioned summary on transmission line sway anomaly detection [20], early warning thresholds are established to serve as the basis for issuing alerts regarding abnormal sway behavior. By establishing warning thresholds, alerts are triggered only when detection results exceed these thresholds. This approach differentiates the severity of abnormal swaying behavior, providing a reliable basis for decision-making regarding the safe operation of transmission lines.

Compare the detection result h_t of abnormal galloping behavior of transmission lines with the actual result to calculate the detection error ς_t between them, and then construct the similarity χ index. Their calculation formulas are respectively:

$$\varsigma_t = \left\| h_t - \vec{h}_t \right\|^2 \tag{17}$$

$$\chi = \frac{1}{1+\varsigma_t} \tag{18}$$

Perform sliding window processing on the similarity sequence, take a specific time period sequence $\overline{\chi}_t = (\chi_1, \chi_2, \cdots, \chi_m)$, integrate it, and calculate the similarity $\tilde{\varsigma}_t$ between abnormal line dancing and normal state within time period t. The formula is as follows:

$$\tilde{\varsigma}_t = \frac{1}{m}\sum_{t=1}^{m}\chi_m \tag{19}$$

m is the width of the sliding window.

Set the abnormal dancing warning threshold Γ for the line based on the results of time period $\tilde{\varsigma}_t$, and the specific formula is:

$$\Gamma = \phi \times \tilde{\varsigma}_t^{\min} \tag{20}$$

In the formula, ϕ is the warning threshold coefficient, and $\tilde{\varsigma}_t^{\min}$ is the minimum similarity value of a normal transmission line.

Warning using Equation (20): When $\tilde{\varsigma}_t = \Gamma$ triggers a clear swing warning; Monitor the swing approaching the critical point at time $\tilde{\varsigma}_t = \Gamma$; There is no warning at time $\tilde{\varsigma}_t = \Gamma$, and the line is normal. This method can monitor the swing intensity in real time.

3. Test Analysis

To comprehensively verify the abnormal swing warning method for transmission lines based on binocular vision, a 110 kV high-voltage transmission line with a total length of 20.4 kilometers and crossing forests and hills in northern China was selected as the test object. The line has strong winds, frequent ice accumulation in winter, and swinging, which is representative of complex environmental conditions.

The experimental system consists of three parts: a binocular image acquisition unit, a data processing platform, and a synchronous monitoring device. It uses a high-resolution industrial camera WSK-TSC620-4G-R, equipped with a 1/1.8 CMOS sensor, with a daytime resolution of 4608×3456 and a nighttime resolution of 1920×1080, a frame rate of 25 fps, a lens focal length of 8mm, and a field of view angle of 77.16° horizontally and 61.3° vertically, which can clearly capture changes in conductor morphology. The camera parallel baseline is installed at the top of the cross arm on the top of the transmission tower, about 28 meters above the ground, facing the central conductor section of the span to cover the obvious flutter zone. The environment of the line is shown in Figure 4, and the parameters are listed in Table 1.

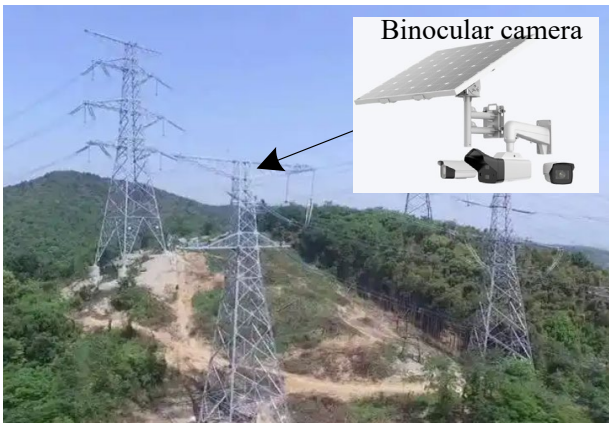

Figure 4. Partial Actual Environment of High Voltage Transmission Lines.

Table 1. Detailed Parameters of Transmission Lines.

Parameter name	Numerical value
Line spacing /m	4~6
Tower distance /m	250~400
Tower height /m	18~35
Tower root opening /m	4
Total width of cross arm /m	7.5
Horizontal bar spacing /m	1.5
Slant support angle /°	45

The data collection period is from November 2023 to February 2024, covering various weather conditions such as icing, strong winds, clear skies, and rainfall during the day and night periods. A total of 2100 valid image samples were obtained, including synchronized left and right images and attitude calibration data. To obtain the true swing state, a high-precision IMU is synchronously installed at the midpoint of the conductor, and the three-dimensional vibration acceleration and angular velocity are recorded as ground truth at a sampling frequency of 100 Hz. Experimental software and hardware configuration: The image processing workstation is equipped with Intel Xeon Gold 6226R CPU and NVIDIA RTX A6000 GPU (48 GB of video memory). The deep learning framework adopts PyTorch 1.12+CUDA 11.6. The edge detection and 3D reconstruction modules are implemented through OpenCV 4.5 and MATLAB 2022a. The algorithm runs on Ubuntu 20.04 system. The parameters of the stereo camera system are shown in Table 2.

Table 2. Parameters related to binocular vision cameras.

Parameter name	Numerical value
Model	WSK-TSC620-4G-R
Vertical rotation angle	70
Image sensor	1/1.8 COMS
Daytime image resolution	4608×3456
Night image resolution	1920×1080
Sensor Size	1/1.2
Frame rate	Colorful
Color mode	USB3
Data transmission method	USB3
Lens interface	C mouth
Pixel size	5.86um×5.86um
Focal length	8mm
Maximum target surface size	8.8mm×6.6mm(Φ11)
Lens field of view angle	D：90.06°H: 77.16° V：61.3

Before implementing the detection and warning method for abnormal swing of transmission lines, it is necessary to first use mathematical morphology to detect the edges of the lines and extract morphological features. To evaluate the effectiveness of edge detection, this method was used to process random transmission line images, and the results are shown in the edge morphology in Figure 5.

(a) Collected original visual images of transmission lines

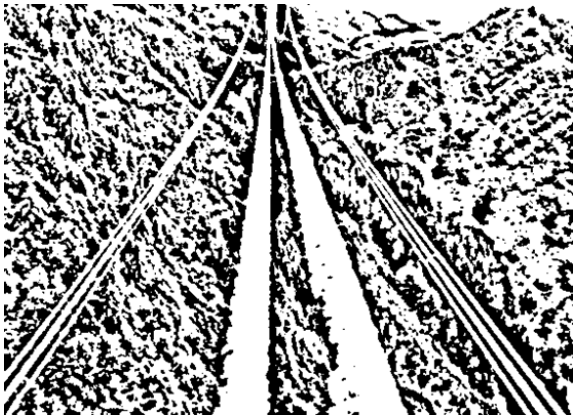

(b) Edge morphology results

Figure 5. Results of Edge Morphology of Transmission Lines

The analysis of Figure 5 shows that the image processing algorithm performs well in power line edge detection. Although the original image (a) has uneven brightness and blurred edges due to severe icing, it is overall clear and can clearly distinguish the wire trajectory from backgrounds such as the sky and forests, laying a good foundation for subsequent processing. The processing result (b) indicates that the edge detection operator based on mathematical morphology successfully extracts the main edge features of the transmission line through operations such as dilation, erosion, and opening and closing, while maintaining the integrity, continuity, and accurate spatial positioning of the edges. The algorithm effectively overcomes the problems of uneven brightness and blurring caused by ice accumulation. The extracted edges have no fractures, uniform width, and correspond to the height of the conductor position in the original image, ensuring the reliability of subsequent flutter anomaly detection. At the same time, the algorithm effectively suppresses noise interference, prevents edge information

misunderstanding or distortion, provides high-quality data for deep learning flutter feature analysis, improves the accuracy and stability of detection models, and has significant engineering value for transmission line safety monitoring under complex meteorological conditions.

To evaluate the effectiveness of the proposed method in detecting abnormal oscillation behavior of transmission lines, random transmission line images captured by a stereo camera system were used for detection, and the results are shown in Figure 6.

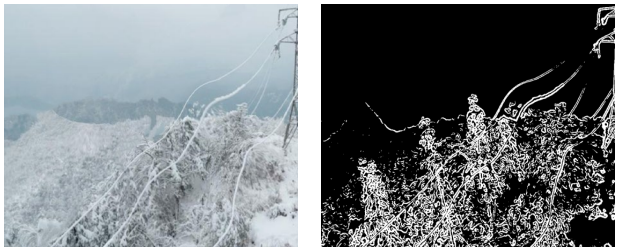

(a1) Left eye camera image

(a2) Edge morphology results

(a3) Feature results after background suppression

(a4) Test results

(a) Left visual image detection results

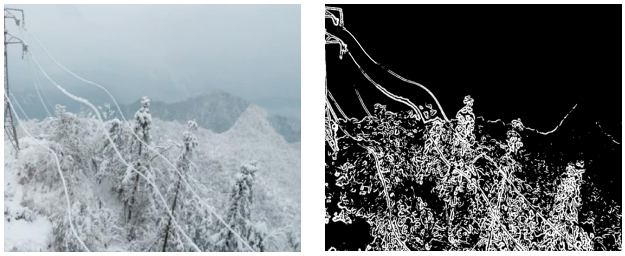

(b1) Right eye camera image

(b2) Edge morphology results

(b3) Feature results after background suppression

(b4) Test results

(b) Right visual image detection results

Figure 6. Detection results of abnormal dancing behaviour of transmission lines

The experiment in Figure 6 shows that the proposed binocular vision method for detecting abnormal swing of transmission lines has significant advantages. It accurately captures swing anomaly features in complex environments through edge and background processing. The system first accurately identifies the edge of the transmission line, suppresses the background, and retains the key features of the conductor. The extraction results of the left and right views are consistent, which is conducive to stereo matching and reconstruction. During detection, the problem conductor segment can be accurately located, and the alignment of the detection frame verifies the accuracy of the system and the correctness of the algorithm. At the same time, it can distinguish between static deformation and dynamic displacement caused by ice accumulation, avoiding misjudgment and improving the detection capability in complex environments. This method combines the advantages of binocular and deep learning to comprehensively capture the shape of the circuit, accurately segment anomalies, and track dynamics. Experiments have shown that it has strong adaptability, can cope with various interferences, and meets the standards for detection accuracy and stability. It provides a reliable solution for monitoring transmission lines and opens up new paths for anomaly detection.

Due to the transient nature of abnormal oscillations in transmission lines, ensuring detection efficiency is crucial for meeting various monitoring and warning requirements. To further validate the performance of the proposed method for detecting abnormal transmission line oscillation, an efficiency score υ is introduced as an evaluation metric to measure the efficiency of the application during detection. The score ranges from 0 to 1, with higher scores indicating better detection efficiency. The calculation formula is as follows:

$$\upsilon = \left(\frac{1-\tau_i}{\sum_{i=1}^{n} \alpha_i} \right) \varphi_i \tag{21}$$

τ_i is the number of iterations of the method, α_i is the network metric involved in efficiency calculation, and φ_i represents the accuracy of the detection result.

By comparing the methods in references [5] and [6], we analyzed the transmission line images collected during daytime and nighttime using these three methods, and obtained the efficiency score υ for detecting abnormal oscillation behavior at different acquisition angles, as shown in Table 3.

Table 3. Efficiency score results for detecting abnormal dancing behaviour of transmission lines

Image category	Collecting angles /°	Reference [5] method	Reference [6] method	Method in the text
Daytime image	15	0.855	0.865	0.966
	30	0.849	0.859	0.958
	45	0.837	0.861	0.961
	60	0.853	0.845	0.959
Night Image	15	0.822	0.863	0.962
	30	0.819	0.821	0.958
	45	0.816	0.814	0.968
	60	0.814	0.802	0.965

Table 3 analysis shows that: (1) In terms of overall effectiveness, the maximum score of methods [5] and [6] does not exceed 0.863 for both daytime and nighttime collection angles. The efficiency score of the proposed method has always been higher, ranging from 0.958 to 0.968, all exceeding 0.95, and the change in image capture angle has the least impact on its performance in detecting abnormal oscillations. It can be seen that the proposed method based on deep binocular vision and ResNet LSTM has the advantages of linear combination and excellent stability in detection efficiency, stronger robustness to changes in viewing angle, and can effectively detect abnormal oscillation of transmission lines at different imaging angles.

(2) In terms of image categories, the efficiency scores of methods [5] and [6] for daytime images are between 0.847-0.855 and 0.855-0.863, respectively, with fluctuations of 0.018 and 0.020; The score of the proposed method ranges from 0.958 to 0.966, and the fluctuation is ≤ 0.008 when the collection angle increases from 15° to 60°. Night-time image acquisition, with scores of 0.814-0.822 and 0.802-0.821 for methods [5] and [6], respectively, with fluctuations of 0.008 and 0.019; The score of the proposed method remains stable between 0.958-0.968, with fluctuations of≤0.010 [5]. The overall efficiency score of the method at night is low and fluctuates little, but it is significantly lower than that during the day [6]. The detection efficiency of the method at night also decreases. The proposed method has stable efficiency scores for detecting abnormal behavior of transmission lines during daytime and nighttime, and has high stability under strong and weak nighttime lighting. It is suitable for harsh environments in the north and can meet the needs of various scenarios.

The proposed method generates flutter anomaly warnings based on the detection results and a predefined alarm threshold (0.60). The warnings are completed by calculating the similarity between the detection and actual results and comparing them with the threshold. The results are shown in Table 4.

Table 4. Warning Results of Abnormal Dance Behaviour of Transmission Lines

Length of transmission line /km	Similarity calculation result	Warning results
2	0.334	Abnormal warning
4	0.466	Abnormal warning
6	0.661	No warning
8	0.552	Abnormal warning
10	0.309	Abnormal warning
12	0.641	No warning
14	0.600	Limit state
16	0.441	Abnormal warning
18	0.297	Abnormal warning
20	0.609	No warning

According to Table 4, this method triggers an alarm by comparing the detection results with a preset threshold (0.60). Six road sections, including 2km and 4km, triggered abnormal alerts, verifying the effectiveness of the warning function. 6 km, 12 km, and other similarities exceeding the threshold road sections, the system correctly did not trigger the alarm. A critical alarm was issued for the 14-kilometer section, and the swing was within a safe range, indicating that it can filter out normal vibrations and improve reliability. The use of dynamic thresholds (such as Equation (20)) can adapt to fluctuations in different routes and accurately identify weak road sections. If the low similarity of the 2-kilometer section triggers the alarm reasonably, and the 6-kilometer section exceeds the threshold but is not triggered and is consistent with the actual situation, it proves that its judgment is accurate and adaptable to complex routes. This mechanism provides a scientific method for detecting abnormal oscillations of transmission lines, which is beneficial for the stable operation of the power grid.

4. Conclusion

To address the challenge of monitoring transmission line sway in adverse weather conditions, this study proposes a warning method based on deep binocular vision to detect abnormal sway. Experiments have shown that it has significant advantages in edge feature extraction, background interference suppression, and swing anomaly detection in complex environments. The main conclusions are as follows:

(1) The binocular vision system obtains three-dimensional data from transmission lines and converts it into two-dimensional images. Combined with

mathematical morphology edge detection operators, it solves the problem of edge detection deviation under adverse conditions. The edge width error is within 0.5 pixels, providing accurate data.

(2) The deep network architecture based on ResNet suppresses complex background interference in morphological edge images and combines an attention mechanism to optimize feature extraction, solving the problem of insufficient feature extraction caused by background noise in traditional methods.

(3) ResNet LSTM hybrid network is used for spatiotemporal modeling of dynamic swaying behavior. Under a dynamic warning threshold of 0.60, it accurately alerts high-risk road sections (similarity 0.297-0.466) and does not alert safe road sections (similarity>0.60), with a detection efficiency of 0.958-0.968 and strong robustness and generalization ability.

This method is reliable for practical engineering applications and can adapt to vibration monitoring of transmission lines under different lighting conditions (day-night difference<0.010) and meteorological conditions (icing, strong winds). In the future, it will optimize the model's lightweight, improve the real-time processing performance of edge computing devices, explore multimodal sensor fusion strategies, and enhance extreme weather monitoring capabilities.

Acknowledgements.

This work was supported by the Science and Technology Project of State Grid Hebei Electric Power Co., Ltd. (grant number: kj2021-013).

References

[1] Jegathesan, V., Jebaseeli, T. J., & David, D. J. Identification of Faults in Invisible Underground Broken Transmission Lines. IETE journal of research. 2023; 69(9):6505-6511.

[2] Sankuri, R. S., Sristy, N. B., & Karri, S. P. K. Syflo: augmenting yolo for real-time health monitoring of electric assets in power transmission lines. Journal of Real-Time Image Processing. 2025; 22(1):1.1-1.15.

[3] Ayambire, P. N., Huang, Q., Awopone, A. K., Jian, L., Anane, P. O. K., & Bamisile, O., et al. A non-contact current traveling wave fault location method for multi-terminal overhead power lines based on adaptive mathematical morphology. Electrical engineering. 2025; 107(1):191-204.

[4] Gonzalez-Fernandez, D., Rezgui, D., De Risi, R., Macdonald, J. H. G., Matsumiya, H., & Titurus, B. Identification and analysis of experiment-driven model for galloping in multi-conductor transmission lines. Engineering structures. 2025; 326:119344.

[5] Fayazi, M., Saffarian, A., Joorabian, M., & Monadi, M. An AI-based fault detection and classification method for hybrid parallel HVAC/HVDC overhead transmission lines. Electric Power Systems Research. 2025; 238:11083.

[6] Shakiba, F. M., Azizi, S. M., Zhou, M., & Abusorrah, A. Application of machine learning methods in fault detection and classification of power transmission lines: a survey. Artificial Intelligence Review: An International Science and Engineering Journal. 2023; 56(7):5799-5836.

[7] Fekri, M., Nikoukar, J., & Gharehpetian, G. B. Vulnerability risk assessment of electrical energy transmission systems with the approach of identifying the initial events of cascading failures. Electric Power Systems Research. 2023; 220:109271.

[8] Garcia-Salguero, M., Dima, E., Mateus, A., & Gonzalez-Jimenez, J. Fast Certifiable Algorithm for the Absolute Pose Estimation of a Camera. SIAM Journal on Imaging Sciences. 2024; 17(3):1415-1432.

[9] Kahnamouei, A. S., & Lotfifard, S. Distribution Systems Fault Location Identification Using Mixed Datasets. IEEE Transactions on Power Delivery. 2025; 40(2):951-964.

[10] Amiri, M. H., Pourgholi, M., Hashjin, N. M., & Ardakani, M. K. Monitoring UAV status and detecting insulator faults in transmission lines with a new classifier based on aggregation votes between neural networks by interval type-2 TSK fuzzy system. Soft computing. 2024; 28(20):12141-12174.

[11] Raju, G. V., & Srikanth, N. V. A novel protection scheme for transmission lines connected to solar photovoltaic and wind turbine farms using fuzzy logic systems and bagged ensemble learning. Electrical engineering. 2024; 106(6):7509-7529.

[12] Mehdi, A., Hassan, S. J. U., & Kim, C. H. Squaring and lowpass filtering data-driven technique for AC faults in AC/DC lines. Electric Power Systems Research. 2023; 223:1.1-1.8.

[13] Sejai, M., Mansouri, A., Bennani, S. D., & Ruichek, Y. Real Time Implementation of Inter-Car Distance Based on an Intelligent Stereovision System for Autonomous Vehicles. International journal of intelligent transportation systems research. 2025; 23(1):525-533.

[14] Fu Q., Kong J. M., Ji Y. F., & Ren F. H. Accurate Stereo Matching for Processing Binocular Vision Image Edge Region. Computer Simulation. 2023; 40(12):226-231.

[15] Ahmad, S., Naeem, F., & Tariq, M. Intelligent Reflective Surfaces Assisted Vehicular Networks: A Computer Vision-Based Framework. IEEE transactions on intelligent transportation systems. 2025; 26(4):4481-4490.

[16] Jeon, Y., Tran, D. Q., Kulinan, A. S., Kim, T., Park, M., & Park, S. Vision-based motion prediction for construction workers safety in real-time multi-camera system. Advanced engineering informatics. 2024; 62:102898.

[17] Bai W.W., Li, J.J., Chen, F. Simulation of Crop Picking Based on Binocular Image Depth Learning. Computer Simulation. 2024; 41(2):187-191.

[18] Gupta, M., Wadhvani, R., & Rasool, A. A real-time adaptive model for bearing fault classification and remaining useful life estimation using deep neural network. Knowledge-based systems. 2023; 259:1-22.

[19] Mirshekali, H., Keshavarz, A., Dashti, R., Hafezi, S., & Shaker, H. Deep learning-based fault location framework in power distribution grids employing convolutional neural network based on capsule network. Electric Power Systems Research. 2023; 223:109529.

[20] Biswas, S., Nayak, P. K., Panigrahi, B. K., & Pradhan, G. An intelligent fault detection and classification technique based on variational mode decomposition-CNN for transmission lines installed with UPFC and wind farm. Electric Power Systems Research. 2023; 223:109526.